Laser Phys. **23** (2013) 075801 (7pp) doi:10.1088/1054-660X/23/7/075801

Laser emission in Nd^{3+} doped barium–titanium–silicate microspheres under continuous and chopped wave pumping in a non-coupled pumping scheme

L L Martín[1], D Navarro-Urrios[2], F Ferrarese-Lupi[3], C Pérez-Rodríguez[1], I R Martín[1,4], J Montserrat[5], C Dominguez[5], B Garrido[3] and N Capuj[6]

[1] Departamento de Fisica Fundamental y Experimental, Electronica y Sistemas, Av Astrofisico Francisco Sanchez, Universidad de la Laguna, E-38206, S/C de Tenerife, Spain
[2] Catalan Institute of Nanotechnology (ICN), Campus UAB, Edifici CM3, E-08193 Bellaterra, Spain
[3] Departament d'Electrònica, Universitat de Barcelona, Carrer Martì i Franquès 1, Barcelona E-08028, Spain
[4] MALTA Consolider Team, Av Astrofisico Francisco Sanchez, Universidad de la Laguna, E-38206, Spain
[5] Instituto de Microelectrònica de Barcelona-CNM-CSIC, Bellaterra, E-08193, Barcelona, Spain
[6] Departamento de Fisica Basica, Av Astrofisico Francisco Sanchez, Universidad de la Laguna, E-38206, Spain

E-mail: lmartin@ull.es

Received 22 February 2013
Accepted for publication 2 April 2013
Published 13 May 2013
Online at stacks.iop.org/LP/23/075801

Abstract
Laser action using non-coupled excitation and detection of microspheres made of Nd^{3+} doped barium–titanium–silicate glass has been demonstrated and measured. The microspheres have also been successfully deposited over Si_3N_4 strip waveguides with a SiO_2 separation layer, thus enabling the laser emission extraction onto a CMOS compatible photonic circuit. The dynamics of the lasing wavelength and intensity has been studied as a function of the pump power and interpreted in terms of thermal effects generated through non-radiative recombination of the excited ions.

(Some figures may appear in colour only in the online journal)

1. Introduction

Optical microcavities are structures where the light is confined into a small volume by means of resonant phenomena. In particular, microdisks, microrings, microtoroids and microspheres use a total internal reflection mechanism that produces the so called whispering gallery mode (WGM) resonances. On fluorescent optical microcavities, the luminescent spectrum of the active material is modulated by the WGM spectrum, which may even enhance the spontaneous emission rate. One of the most direct applications of these structures is in chemical or bio-sensing [1], refractive index sensing and temperature sensing [2, 3], but relevant findings have also been achieved towards using them as all-optical switches [4] and micro-mechanical oscillators [5]. Among all microresonators, the microspheres have some key features: they can be made from many compositions including polymers, crystalline or glassy phases, and they can have ultra-high quality factors (Q) up to 8×10^9 [6], which means a very high storage time of the light in the resonant cavity.

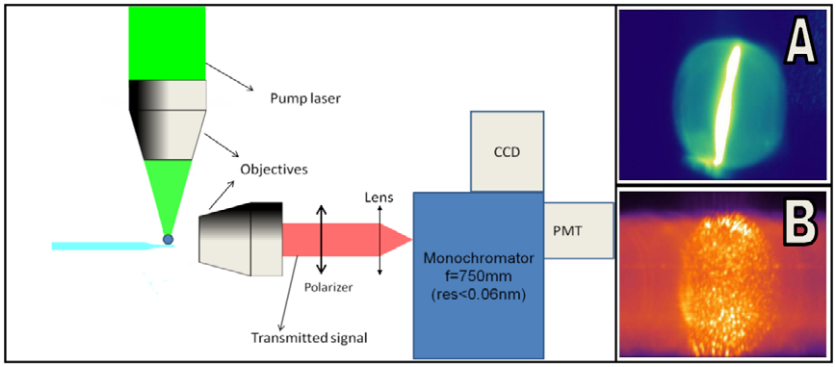

Figure 1. Left: experimental scheme employed in the experiments. The microsphere is positioned over a glass tip, pumped by the top green laser. Signal is collected by the right side microscope objective and focused in the entrance of a spectrograph. Right: false colour images of fluorescence induced by the pumping beam across the sphere at zero order of the grating (A) and spectral image of a lasing sphere showing the speckles of the scattered laser light, centred at about 1065 nm (B). Both images are vertically elongated by optical defects.

The possibility of using micron sized, spherical particles as resonators has been studied since the early days of lasers. If a microsphere is doped with a high enough concentration of rare earth ions, it creates an active cavity which acts as both the gain medium and the resonant cavity for the laser emission. During recent years, there has been an enormous industrial interest in microscaled lasers with a broad spectrum of applications, such as intrachip telecom and lab-on-a-chip sensors. The idea of using spherical particles for laser emission was first investigated by Garret *et al* [7] using CaF_2 spheres doped with samarium ions. The first laser action in a solid-state sphere was demonstrated by Baer [8] using Nd:YAG spheres with a diameter of 5 mm. Recently, laser emission has been achieved at visible and NIR wavelengths on various rare earth doped glass microspheres, from cryogenic [9] to room temperature in silica [10, 11], ZBNA [12], or phosphate [13] glasses, using Nd^{3+} or Er^{3+} ions as gain dopant.

The coupling of laser microspheres to Si_3N_4 waveguides coated with SiO_2 is a step towards the practical use of the microsphere–waveguide combination as integrated lasers or sensors due to the excellent properties of these waveguides in terms of low scattering losses, no absorption losses and compatibility with Si technology [14].

Recently, the barium–titanium–silicate (BTS) glass has been studied and converted into a glass–ceramic with high non-linear coefficients [15] by conventional thermal treatment or by laser heating [16]. A further interesting property is that the BTS material can be fabricated in a way that combines glass phase and nanocrystalline phases. In this work we have focused our studies on the glass phase and obtained laser action in BTS microspheres doped with Nd^{3+} under direct excitation. Moreover, in spite of the previous papers that usually limit the studies to microspheres coupled to tapered fibres or waveguides, the detection of the laser emission has been carried also using a non-coupled system. The thermal behaviour of the optical properties of microsphere resonators has been studied previously [17, 18]. However, the laser intensity and its dynamics were not regarded, which is one of the main goals of this work.

2. Experimental details

The microspheres were produced from a BTS glass with the composition of 40%BaO–20%TiO_2–40%SiO_2 and doped with 1.5% Nd_2O_3 (in the molar ratio). Commercial powders of ACS reagent grade (purity $\geq$ 99.9%) $BaCO_3$, TiO_2, SiO_2, and Nd_2O_3 were mixed and melted in a platinum–rhodium crucible at 1500 °C for one hour in an electric furnace. After this, the melt was poured between bronze plates following the melt-quenching method.

Microspheres can be made by different methods; these include polishing, chemical etching and rapid quenching of liquid droplets. In this work, the microspheres are fabricated by the method exposed by Elliot *et al* [19] from the precursor glass mentioned above. Using this technique, microspheres of diameters ranging from 10 to 100 μm were obtained.

The experimental setup used is schematized in figure 1. The collection setup consists of a microscope objective (NA = 0.4) placed on an *xyz* stage. A linear polarizer is placed just after the objective in the collimated beam region. The signal is focused onto the entrance slit of a 3/4 m spectrograph, with two exit ports, CCD camera or photomultiplier (PMT). The whole collection system allows a maximum resolution of about 0.06 nm. Indeed, since the sample holder possesses an independent *xyz* movement, it is possible to situate the region of the microspheres to be analysed at the centre of the entrance slit. As previously studied [20], the air–sphere interface is the best zone to observe the resonances corresponding to the WGM. The setup presents the particularity of efficiently collecting the emitted signal, not only within a reduced solid angle around the collection axis direction (given by the NA of the objective), but also of a small physical volume. The importance of analysing a reduced region of the emitting microsphere has been pointed out recently [21], revealing that different resonance positions and quality factors can be observed depending on the analysed zone.

In order to excite the Nd^{3+} ions, we have employed the 514 nm line of an Ar^+ ion laser, which is absorbed by the $^4I_{9/2} \rightarrow {}^4G_{9/2}$ transition of Nd^{3+} ions. This wavelength increases the thermal effects regarding the most common

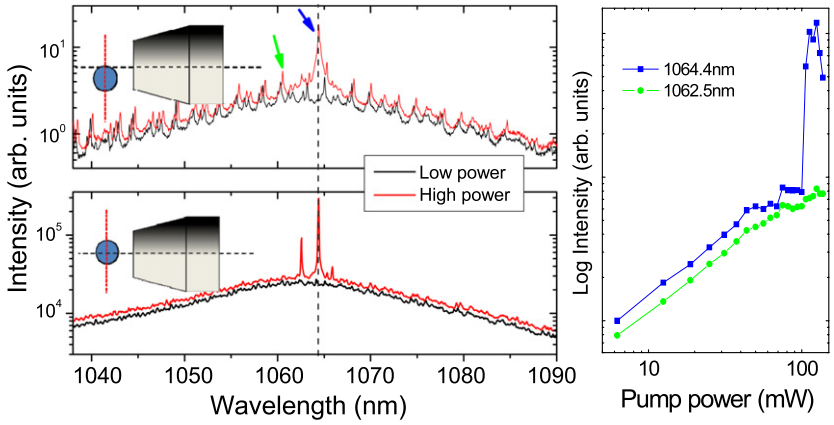

Figure 2. Left: spectra obtained at low pump power (90 mW, black curves) and high pump power (125 mW, red curves). The top (bottom) panel shows the results when collecting from the lateral (central) part of the microsphere. The collection objective positions with respect to the microsphere for both cases are also illustrated. Right: dependence of the intensity of at $\lambda = 1064.4$ nm (blue arrow in top left) and at $\lambda = 1058.3$ nm (green arrow in top left).

808 nm used to pump directly the $^4I_{9/2} \rightarrow {}^4F_{5/2}$ transition. The pump laser is focused on the top of a single microsphere by means of a long working distance and low NA objective, which provides a spot size of few micrometres and a power flux about 10^4 W cm^{-2}. The exact pumping zone can also be micro-controlled independently. A previous study [20] revealed that the centre of the sphere is the best zone to pump the resonances. To study the dynamics of the thermal effects on the emission of the microsphere, a mechanical chopper was added to the pump laser.

For the non-coupled experiments, microspheres were positioned on the top of a glass tip. We have also positioned the microspheres over a buried strip Si_3N_4 waveguide fabricated with standard CMOS procedures embedded in SiO_2, which was used for extracting the laser light. The separation of the SiO_2 layer among the sphere and the waveguides is about 150 nm. The diameter of the microspheres studied in this work is in the 45–55 μm range and their measured quality factor is limited by the resolution of our setup, i.e. at least 10^4.

3. Results and discussion

In figure 1 (right) (A) it is shown the zero order image of the sphere obtained by filtering out the pumping laser. It shows an intense fluorescence in the pumping laser path corresponding to the broad Nd^{3+} bands centred on wavelengths 810, 890 and 1060 nm. At high enough pumping powers, lasing action has been observed, which is illustrated in figure 1 (right) (B) with an image of the microsphere at a lasing wavelength ($\lambda_{las} = 1065$ nm). This image has been obtained by tuning the spectrograph to λ_{las} and opening the input spectrograph slit to its maximum width. It is worth noting that the resolution of the spectrograph under these conditions ($\sim$2 nm) allows the spectral isolation from other lasing modes.

In figure 2 (left), the two curves of the bottom panel show the spectra obtained when observing the central region of the microsphere at a pump power below laser threshold (LT) in black (90 mW) and at a pump power above LT in red (125 mW). To obtain this, the focus of the collection objective is at the physical centre of the sphere and only a reduced emitting volume around this point is collected. The black line shows the typical measured emission spectrum corresponding to the well known $^4F_{3/2} \rightarrow {}^4I_{11/2}$ transition of Nd^{3+} ions randomly located within a BTS glass. This signal is mainly associated with direct emission towards the objective. At high pump power, two narrow peaks corresponding to laser light at 1064.4 and 1062.5 nm are collected thanks to a scattering process occurring within the microsphere. This result is similar to that of Murugan *et al* [22] when they collect from the top and side of the microsphere. It is also consistent with the image of figure 1 (right) (B), in which scattering processes illuminate the whole sphere volume with laser light.

In the top panel of figure 2, the curves illustrate the situation when collecting the light emitted from the boundary of the microsphere (the focus of the objective is the same as in the previous case, but the emitting volume is centred on the sphere boundary). When the ions are embedded in the glass microsphere, their emission band is modulated with the resonant spectral features typical of photonic circular cavities, i.e. the WGMs, giving rise to the spectra shown in this panel. In this case, the signal associated with the WGMs is mainly due to the radiative loss mechanism of WGMs with wavevectors aligned with the collection axis. As previously, the black line shows the spectrum below LT (90 mW) while the red line the spectrum above LT (125 mW). The units of the top and bottom panels are consistent and show that much more laser light can be received from the central part of the microsphere. The laser wavelength matches in both configurations but does not fit with any of the WGMs observed at low pump power, even taking into account the spectral shift observed in the WGMs at high powers due to thermal effects. Both facts indicate that the laser light collected in this configuration is also a result of a scattering process. Moreover, we can conclude that the laser mode is originally built up within a WGM following a circular trajectory in a different plane from those allowed by the

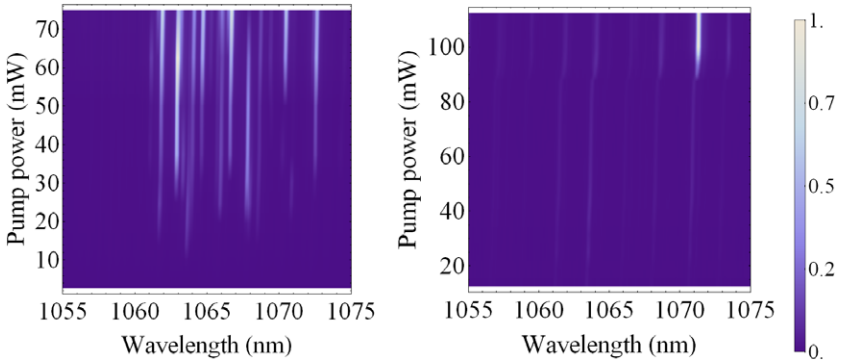

Figure 3. Emission spectra of microspheres at various chopped pump powers. The chopper frequency is 75 Hz and the duty cycle 50%. Only the resonances showing bright laser emission are visible on the graphs. Left: free air sphere showing a multimode laser. Right: sphere coupled to a Si_3N_4 waveguide showing a single mode laser.

collection system. In a previous work [21], we demonstrated that the passive losses can present different values depending on the orientation of the plane in which the trajectory of the mode is contained, directly impacting in the Q of the WGM. Thus, WGMs embedded in a trajectory with high Q are more favoured to support a lasing mode than one with lower Q. Apart from this, it also has to be taken into account that the pumping laser efficiency over the sphere volume is not uniform, which certainly will favour certain trajectories over others.

The significant spectral deviation of the lasing wavelength with respect to the closest WGM could be explained in terms of two different causes that are compatible with our observations. First, the microsphere presents a certain degree of ellipticity, so the WGM originating the laser action follows an optical path different from that of the WGM of the same order that is efficiently collected. On the other side, the high local intensity within the volume covered by the lasing mode originates changes in the refractive index associated with second order non-linear effects.

By analysing the behaviour of the signal intensity at a lasing wavelength with the pumping power (shown on figure 2 (right)) the LT power is obtained. Indeed, an LT of about 100 mW has been extracted at the lasing wavelength $\lambda = 1064.4$ nm (blue arrow in figure 2 (left) top), which is similar to what is observed for other lasing resonances. It is worth mentioning that the signal below LT has a different origin than that observed above LT. Instead, for a resonance placed at $\lambda = 1058.3$ nm (green arrow in figure 2 (left)) no laser action occurs and a sublinear behaviour with power is observed for the analysed power range. Moreover, it is remarkable that the intensity of the laser emission decreases at pump powers well above LT. This result could be explained on the basis of the increment of non-radiative decay channels due to the heating of the microsphere. This effect can be strongly reduced by changing the pump wavelength to about 808 nm in order to pump directly the $^4F_{3/2}$ electronic level and avoiding the extra energy being lost as heat. In fact, a strong reduction of the LT would be expected together with an increase of the absolute emitted power.

The maximum intensity measured at the laser wavelength when collecting from the centre corresponds to a power of about 10 μW. Nevertheless, since in this configuration we are not efficiently collecting the laser signal, the actual emitted power must be orders of magnitude higher.

In figure 3, the two graphs show the emission spectra of microspheres at various pump powers using a chopped pump at 75 Hz (duty cycle of 50%). Due to the linear character of the colour scale, only the laser emissions are clearly visible. The left graph corresponds to a free air sphere and the right one to a sphere coupled to a buried Si_3N_4 rib-waveguide.

On the free air sphere (left) it can be seen that the LT is about 20 mW at 1063 nm, which is nearly five times lower LT than in the case of a continuous wave pump (about 100 mW). The multimode laser emission at pump powers above 30 mW is also very clear. We will demonstrate in the following that the decrease of the LT with frequency is related to a decrease of the average temperature of the sphere, leading to an attenuation of the efficiency of non-radiative recombination mechanisms.

In the right graph, the coupled microsphere shows a higher LT of about 90 mW. The significantly higher LT observed for the coupled spheres is probably a consequence of a strong decrease of the overall quality factor (Q) of the coupled structure due to an overcoupling to the waveguide [23], i.e. the gap distance is too small. For the same reason, under continuous wave experiments the coupled system does not show laser emission at reasonable pump powers (<300 mW). The LT might not even be reached by further increasing the pump power, since, as we will show later, thermal effects reduce the light emission efficiency at the expense of non-radiative recombination mechanisms.

For the particular case shown on the right graph, we have observed only a single laser mode. In other coupled spheres, double mode lasing has also been observed. In any case, far fewer laser modes can be observed in comparison to the free air spheres. The main reason is twofold. On the one hand, the quality factor has been harmed by the presence of the waveguide and the conditions for lasing are more restrictive. On the other hand, only laser modes whose evanescent field couples to the waveguide modes can be seen at the waveguide output. In other words, similarly to what is reported in [22], the sphere might be lasing in other modes, probably with lower LT, that are not coupled to the buried waveguide.

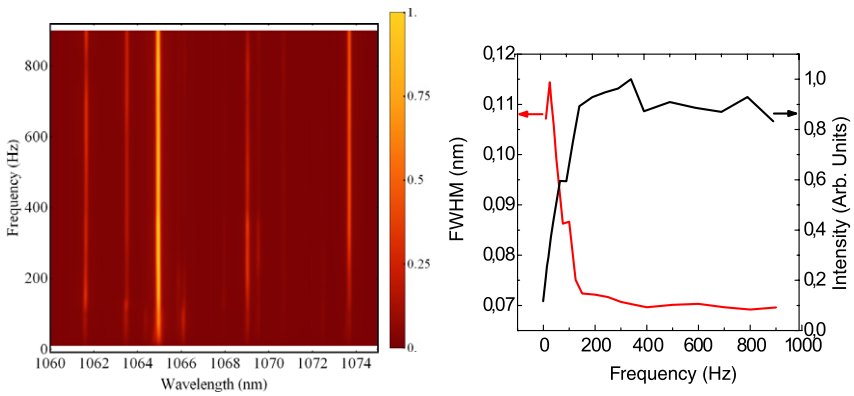

Figure 4. Left: graph showing the spectra for the multimode laser region for a free air sphere, at different chopper frequencies, while keeping the pump power constant. The colour bar shows the normalized intensity. Right: dependence of the intensity (black) and FWHM (red) with the chopper frequency of the 1065 nm laser resonance.

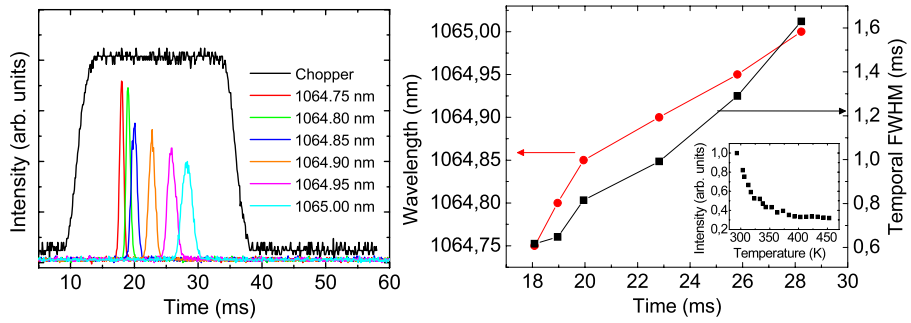

Figure 5. Left: dependence of the intensity on time for different wavelengths. The blue curve is the chopper signal and the narrow peaks are the laser signal at different wavelengths. Right: temporal dependence of the wavelength and of the temporal FWHM of the left graph. Inset: integrated intensity of the $^4F_{3/2} \rightarrow {}^4I_{9/2}$ transition obtained in a bulk sample calibrated with temperature under c.w. excitation.

As shown previously, chopping the pump laser reduces the LT of the microspheres. In order to have more insight into this effect, we have studied the behaviour of the laser emission with the chopper frequency at a fixed pump power of 125 mW, and integrating for enough time to average over multiple cycles (shown in figure 4). The plot shows a multimode emission with laser resonances from 1060 to 1075 nm; it can be seen that the intensity of the emission is not independent of the frequency, as could be expected for a constant pump power. The black curve of the right panel plots the detailed intensity of the brightest laser resonance at 1065 nm, where it is clear that it monotonically increases up to stabilization at 200 Hz. As the pump power remains constant in this experiment and the output intensity increases about ninefold, the efficiency of the emission is increased by about one order of magnitude only by optimizing the chopper frequency. The red curve represents the full width at half maximum (FWHM) of the resonance, showing a line narrowing with frequency down to the resolution limit. It is worth mentioning that the effects for the chopping frequency on the spectral content of Nd^{3+} doped chalcogenic laser microspheres have already been noted [24], but not studied in depth.

On the other hand, time resolved measurements on a bulk glass sample allowed extraction of a radiative lifetime of about 110 μs at room temperature, which is 50 times shorter than the illumination time of a 200 Hz signal. Also, the cavity-lifetime or storage time of the highest quality microspheres reported ($Q = \omega\tau_{\text{storage}} = 10^8$) can be at most of the order of 50 ns, while our resonator at $Q = 14\,000$ would have a storage time of about 5 ps. This means that, at the studied frequency of 200 Hz, it can be considered to be working on stationary conditions both for the emitting material and for the geometrical cavity.

Thus, the possible explanation for the results shown in figure 4 is found in the temporal variations of the sphere temperature. Indeed, the FWHM of the resonance is a result of an inhomogeneous broadening due to a relatively slow process (in the millisecond range) of temperature stabilization in which the optical path of the observed mode changes during the pump pulse. These changes can be associated with modifications in the refractive index, in the sphere radius or in both [18]. Concerning the increase of the lasing signal with frequency, it seems clear that it reflects an improvement of the emission efficiency since the measured Q value is not affected by the temperature. Therefore, the decrease of the LT with frequency is mainly ascribed to a decrease of the average temperature of the sphere, and therefore to an attenuation of the radiative emission efficiency quenching due to the presence of non-radiative recombination mechanisms.

Time resolved measurements have been made in order to confirm our hypothesis regarding the effect of the pump laser frequency on Q and on the lasing wavelength. Figure 5

(left) shows the temporal evolution of the laser light under a 20 Hz pump. The different curves correspond to the temporal evolution of the emitted signal at fixed wavelengths. We can conclude the following.

(i) The wavelength of the laser emission redshifts as a function of the delay time with respect to the starting point of the pump pulse. This is compatible with a thermal expansion of the microsphere and an increase of the material refractive index, which is the normal behaviour of a BTS glass [18].

(ii) There is a slow decrease of the maximum intensity with time. This is explained in terms of the quenching of the emission signal produced by the increase of non-radiative recombination assisted by phonons, which is enhanced with the temperature. The calculated change in temperature produces a decrease in the emission efficiency of about 60% (inset of figure 5 (right)), which is consistent with that observed in figure 5 (left). Indeed, the inset of figure 5 (right) shows the decrease of the $^4F_{3/2} \rightarrow {}^4I_{9/2}$ transition integrated intensity as a function of the temperature for a bulk sample of Nd^{3+} doped BTS glass. It is worth noting that the latter measurement was carried out at constant pump power inside an electric furnace with temperature control.

(iii) The redshift speed decreases as a function of time. The black curve of figure 5 (right) shows the temporal FWHM (t-FWHM) of the laser signal as a function of time for a fixed wavelength. The t-FWHM is inversely proportional to the speed of the laser spectral shift during the pump pulse, which is at the same time associated with the temperature increase. This speed is higher at the beginning and lower at the end of the pumping pulse due to stabilization of temperature. The red curve of figure 5 (right) shows the lasing wavelength as a function of time, where a sort of saturation is appreciated for longer times. We have fitted the latter curve with an exponential law and extracted a stabilization wavelength of 1065.05 nm with a typical stabilization time (time to reach the $1/e$ of the total wavelength shift) of about 7 ms. This stabilization speed is of the same order to the value measured independently by Carmon [24] and Lin [10] in silica microspheres.

According to a previous work [18], a wavelength shift of 11 pm K^{-1} is expected for this material and a similar microsphere size. From the exponential fit of the experimental curve we can extract a total wavelength shift of 0.85 nm, which indicates that due to the laser heating the temperature has been increased by 77 K at 125 mW.

4. Conclusions

Laser emission has been achieved and studied on Nd^{3+} doped BTS glass microspheres with diameters of about 50 μm. We have studied microspheres both in an isolated configuration and vertically coupled to Si_3N_4 strip waveguides fabricated using CMOS compatible techniques. The laser intensity and its power efficiency were studied in terms of the pump power and temporal chopping frequency. The laser thresholds found are to be about 100 mW for an isolated microsphere under a continuous wave pump and 20 mW under a 300 Hz chopped pump. The microspheres coupled to the strip waveguides do not present laser emission on the continuous wave pump at pump power lower than 300 mW, but showed an LT of 125 mW at the 300 Hz chopped pump.

The decrease of LT with chopper frequency is directly associated with a diminution of the average temperature of the microspheres.

We have analysed the temporal behaviour of the wavelength position and the intensity of the lasing emission and extracted a redshift and a diminution of the intensity respectively. These phenomena have been explained in terms of thermal processes originated by the non-radiative recombination of the excited ions.

Acknowledgments

The authors thank the Ministerio de Economía y Competitividad of Spain (MINECO) within the National Program of Materials (MAT2010-21270-C04-02/-03/-04), the Consolider-Ingenio 2010 Program (MALTA CSD2007-0045, www.malta-consolider.com), the EU-FEDER, the GICSERV NGG-268 for their financial support and ACIISI of Gobierno de Canarias for the project ID20100152 and FPI. DN-U acknowledges the financial support of Generalitat de Catalunya through the Beatriu de Pinòs program.

References

[1] Vollmer F and Arnold S 2008 Whispering-gallery-mode biosensing: label-free detection down to single molecules *Nature Methods* **5** 591–6

[2] Hanumegowda N M, Stica C J, Patel B C, White I and Fan X D 2005 Refractometric sensors based on microsphere resonators *Appl. Phys. Lett.* **87** 201107

[3] Dong C H, He L, Xiao Y F, Gaddam V R, Ozdemir S K, Han Z F, Guo G C and Yang L 2009 Fabrication of high-*Q* polydimethylsiloxane optical microspheres for thermal sensing *Appl. Phys. Lett.* **94** 231119

[4] Roy S, Prasad M, Topolancik J and Vollmer F 2010 All-optical switching with bacteriorhodopsin protein coated microcavities and its application to low power computing circuits *J. Appl. Phys.* **107** 053115

[5] Bahl G, Zehnpfennig J, Tomes M and Carmon T 2011 Stimulated optomechanical excitation of surface acoustic waves in a microdevice *Nature Commun.* **2** 403

[6] Vahala K J 2003 Optical microcavities *Nature* **424** 839–46

[7] Garrett C G, Kaiser W and Bond W L 1961 Stimulated emission into optical whispering modes of spheres *Phys. Rev.* **124** 1807–9

[8] Baer T 1987 Continuous-wave laser oscillation in a Nd–YAG sphere *Opt. Lett.* **12** 392–4

[9] Treussart F, Ilchenko V S, Roch J F, Domokos P, Hare J, Lefevre V, Raimond J M and Haroche S 1998 Whispering gallery mode microlaser at liquid helium temperature *J. Lumin.* **76/77** 670–3

[10] Lin G, Tillement O, Candela Y, Martini M, Cai Z, Lefevre-Seguin V and Hare J 2010 *Proc. SPIE* **7716** 771622

[11] Cai M, Painter O, Vahala K J and Sercel P C 2000 Fiber-coupled microsphere laser *Opt. Lett.* **25** 1430–2
[12] Shortt B, Carey R and Chormaic S N 2005 Opto-Ireland 2005: Photonic Engineering *Proc. SPIE* **5827** 47
[13] Dong C H, Yang Y, Shen Y L, Zou C L, Sun F W, Ming H, Guo G C and Han Z F 2010 Observation of microlaser with Er-doped phosphate glass coated microsphere pumped by 780 nm *Opt. Commun.* **283** 5117–20
[14] Daldosso N, Melchiorri M, Riboli F, Sbrana F, Pavesi L, Pucker G, Kompocholis C, Crivellari M, Bellutti P and Lui A 2004 Fabrication and optical characterization of thin two-dimensional Si_3N_4 waveguides *Mater. Sci. Semicond. Process.* **7** 453–8
[15] Masai H, Tsuji S, Fujiwara T, Benino Y and Komatsu T 2007 Structure and non-linear optical properties of $BaO–TiO_2–SiO_2$ glass containing $Ba_2TiSi_2O_8$ crystal *J. Non-Cryst. Solids* **353** 2258–62
[16] Martin L L, Haro-Gonzalez P, Martin I R, Puerto D, Solis J, Caceres J M and Capuj N E 2010 Local devitrification of Dy^{3+} doped $Ba_2TiSi_2O_8$ glass by laser irradiation *Opt. Mater.* **33** 186–90
[17] Carmon T, Yang L and Vahala K J 2004 Dynamical thermal behavior and thermal self-stability of microcavities *Opt. Express* **12** 4742–50
[18] Martin L L, Perez-Rodriguez C, Haro-Gonzalez P and Martin I R 2011 Whispering gallery modes in a glass microsphere as a function of temperature *Opt. Express* **19** 25792–8
[19] Elliott G R, Hewak D W, Murugan G S and Wilkinson J S 2007 Chalcogenide glass microspheres; their production, characterization and potential *Opt. Express* **15** 17542–53
[20] Martin L L, Haro-Gonzalez P, Martin I R, Navarro-Urrios D, Alonso D, Perez-Rodriguez C, Jaque D and Capuj N E 2011 Whispering-gallery modes in glass microspheres: optimization of pumping in a modified confocal microscope *Opt. Lett.* **36** 615–7
[21] Navarro-Urrios D, Baselga M, Lupi F F, Martin L L, Perez-Rodriguez C, Lavin V, Martin I R, Garrido B and Capuj N E 2012 Local characterization of rare-earth-doped single microspheres by combined microtransmission and microphotoluminescence techniques *J. Opt. Soc. Am.* B **29** 3293–8
[22] Murugan G S, Zervas M N, Panitchob Y and Wilkinson J S 2011 Integrated Nd-doped borosilicate glass microsphere laser *Opt. Lett.* **36** 73–5
[23] Gorodetsky M L and Ilchenko V S 1999 Optical microsphere resonators: optimal coupling to high-Q whispering-gallery modes *J. Opt. Soc. Am.* B **16** 147–54
[24] Elliott G R, Murugan G S, Wilkinson J S, Zervas M N and Hewak D W 2010 Chalcogenide glass microsphere laser *Opt. Express* **18** 26720–7